Am J Physiol Regul Integr Comp Physiol 295: R979–R990, 2008.
First published June 25, 2008; doi:10.1152/ajpregu.00192.2008.

Regulation of pyruvate dehydrogenase in the common killifish, *Fundulus heteroclitus*, during hypoxia exposure.

Jeffrey G. Richards,[1] Brian A. Sardella,[2] and Patricia M. Schulte[1]

[1]*Department of Zoology, The University of British Columbia, Vancouver, British Columbia, Canada; and* [2]*Department of Animal Science, University of California Davis, Davis, California*

Submitted 16 March 2008; accepted in final form 23 June 2008

Richards JG, Sardella BA, Schulte PM. Regulation of pyruvate dehydrogenase in the common killifish, *Fundulus heteroclitus*, during hypoxia exposure. *Am J Physiol Regul Integr Comp Physiol* 295: R979–R990, 2008. First published June 25, 2008; doi:10.1152/ajpregu.00192.2008.—We examined the metabolic responses of the hypoxia-tolerant killifish (*Fundulus heteroclitus*) to 15 h of severe hypoxia and recovery with emphasis on muscle substrate usage and the regulation of the mitochondrial protein pyruvate dehydrogenase (PDH), which controls carbohydrate oxidation. Hypoxia survival involved a transient activation of substrate-level phosphorylation in muscle (decreases in [creatine phospate] and increases in [lactate]) during which time mechanisms to reduce overall ATP consumption were initiated. This metabolic transition did not affect total cellular [ATP], but had an impact on cellular energy status as indicated by large decreases in [ATP]/[ADP_{free}] and [ATP]/[AMP_{free}] and a significant loss of phosphorylation potential and Gibbs free energy of ATP hydrolysis ($\Delta fG'$). The activity of PDH was rapidly (within 3 h) decreased by ~50% upon hypoxia exposure and remained depressed relative to normoxic samples throughout. Inactivation of PDH was primarily mediated via posttranslational modification following the accumulation of acetyl-CoA and subsequent activation of pyruvate dehydrogenase kinase (PDK). Estimated changes in cytoplasmic and mitochondrial [NAD^+]/[NADH] did not parallel one another, suggesting the mitochondrial NADH shuttles do not function during hypoxia exposure. Large increases in the expression of PDK (PDK isoform 2) were consistent with decreased PDH activity; however, these changes in mRNA were not associated with changes in total PDK-2 protein content assessed using mammalian antibodies. No other changes in the expression of other known hypoxia-responsive genes (e.g., lactate dehydrogenase-A or -B) were observed in either muscle or liver.

Gibbs free energy; pyruvate dehydrogenase kinase; energy charge; Gibbs free energy; muscle; fish

THE ABILITY TO SUPPRESS CELLULAR ATP DEMAND to match the limited capacity for oxygen-independent ATP production has emerged as the unifying adaptive strategy ensuring hypoxia survival (19). In hypoxia-tolerant animals, reductions in cellular ATP demand are achieved through the controlled arrest of processes involved in membrane ion movement (8, 40), protein synthesis (28, 56), RNA transcription, urea synthesis, gluconeogensis, and other anabolic pathways (19). The cellular signals that initiate the hypoxia-induced decrease in oxygen demand are not known. However, work in aestivating snails (3) suggests that the signal for metabolic rate depression originates from the mitochondria and is controlled to a great degree by changes in the kinetics of substrate oxidation (4, 14, 15, 46). Mitochondria isolated from skeletal muscle of hypoxia-acclimated frogs (*Rana temporaria*) show reduced *state III* and *IV* respiration rates, increased mitochondrial oxygen affinity (47), and reduced electron transport chain activity (46) compared with mitochondria isolated from normoxia-exposed animals. This ability to effectively arrest mitochondrial function during hypoxia exposure is essential to limit the production of harmful reactive oxygen species (ROS) and prevent mitochondrial-mediated initiation of apoptosis (32). The mechanistic basis for mitochondrial arrest is not known, but it has been suggested (49) that the mitochondrial protein complex pyruvate dehydrogenase (PDH) is involved in mediating metabolic rate depression.

PDH is the rate-limiting enzyme that regulates the rate of entry of glycolytically derived pyruvate into the TCA cycle and mitochondrial oxidative metabolism (20) and is regulated by both product inhibition (NADH and acetyl-CoA) and reversible covalent modification (phosphorylation/dephosphorylation). The transformation of PDH between the active form (PDHa) and inactive form is regulated by the relative activities of pyruvate dehydrogenase kinase (PDK), which phosphorylates PDH to deactivate it, and PDH phosphatase, which activates PDH by dephosphorylation (42). PDH kinase is activated by metabolite concentrations signaling a high cellular energy status (high [acetyl-CoA]/[free-CoA], [ATP]/[ADP_{free}] and low pyruvate and [NAD^+]/[NADH]) (20). Expression of PDK in mammalian cell lines, in particular the PDK-1 isoform, is hypoxia responsive and regulated by the transcription factor hypoxia inducible factor-1 (HIF-1) (10). Increases in PDK-1 mRNA during hypoxia exposure has been linked to the phosphorylation of PDH, reduced mitochondrial oxygen consumption, and ROS generation (33, 43). Expression of PDK-1 in HIF-1α null lymphoma cells resulted in increases in cellular [ATP], an attenuation of hypoxic ROS generation, and a lack of hypoxia-induced apoptosis during severe hypoxia exposure (24). Thus, the regulation of PDK appears to be an important aspect of hypoxia cell survival even in hypoxia-intolerant mammalian cells; however, few studies have examined the regulation of PDH and PDK in animals that have evolved to survive hypoxia exposure. Richards et al. (40) demonstrated a modest decrease in muscle PDH activity in the hypoxia-tolerant Amazonian cichlid (*Astronotus ocellatus*) but the detailed mechanisms regulating PDH during hypoxia are not known in any hypoxia-tolerant animals.

Here we characterize metabolic responses of the hypoxia-tolerant killifish (*Fundulus heteroclitus*) to 15-h severe hypoxia

Address for reprint requests and other correspondence: J. G. Richards Dept. of Zoology, The Univ. of British Columbia, 6270 Univ. Blvd., Vancouver, BC, Canada V6T 1Z4 (e-mail: jrichard@zoology.ubc.ca).

The costs of publication of this article were defrayed in part by the payment of page charges. The article must therefore be hereby marked "*advertisement*" in accordance with 18 U.S.C. Section 1734 solely to indicate this fact.

exposure followed by 12-h recovery in normoxic water. Killifish inhabit estuaries along the east coast of North America that undergo diel and seasonal fluctuations in dissolved oxygen. Diel fluctuations in oxygen are caused by plant and animal respiration at night when no photosynthesis occurs to replenish dissolved oxygen. As a result of the environmental fluctuations in dissolved oxygen, killifish have evolved an amazing suite of adaptations to enhance hypoxia survival including modifications to behavior (48) and biochemical and molecular responses (25, 37). In *F. grandis*, long-term hypoxia exposure led to tissue-specific phenotypes in metabolic capacity with an upregulation in glycolytic capacity (i.e., increases in enzyme activities) in liver and decreases in muscle (29). Taken together, these data suggest that muscle severely reduces ATP utilization during hypoxia exposure, in part through reductions in motor activity, and therefore we focused on the muscle in the present study to determine whether PDH modulation was associated with hypoxic survival. Specifically, we examined the activity of PDH in muscle of killifish during hypoxia exposure and examined the factors that regulate PDH activity, including changes in allosteric modulators (e.g., [ATP]/[ADP_{free}], [NAD^+]/[NADH] ratios, [pyruvate]) and the patterns of PDK mRNA expression in an attempt to elucidate the importance of PDH regulation in hypoxia survival in the hypoxia-tolerant killifish.

METHODS AND MATERIALS

Animals

Adult killifish (*F. heteroclitus heteroclitus* L.; weighing 3.1 ± 0.13 g wet weight; mean ± SE) were captured from New Brunswick, Canada and transported to the University of British Columbia and housed indoors in aquaria with filtered synthetic brackish water (10 g/l; Deep Ocean, Carson, CA) made up in dechlorinated City of Vancouver tap water. Water temperature was maintained at 20°C, and oxygen partial pressure was ~160 Torr. Fish were held under these conditions for at least 30 days before experimentation. Fish were fed commercial trout chow (PMI Nutrition International, Brentwood, MO) at ~2% body wt/day. All experimental procedures were conducted according to the guidelines set out by the Canadian Council for Animal Care administered by the University of British Columbia Animal Care Committee and were approved by the University of British Columbia Animal Care Committee.

Gene Identification and Sequencing

Tissue sampling and RNA extraction. Adult killifish were taken directly from their holding tanks and killed by concussion; samples of brain, gill, intestine, liver, muscle, spleen, and heart were immediately dissected and frozen in liquid nitrogen. Samples were stored at −80°C until RNA extraction. Total RNA was extracted from tissues using the guanidinium thiocyanate method outlined by Chomczynski and Sacchi (9) using TriPure Isolation Reagent (Roche Diagnostics, Montreal, QC, Canada). Total RNA was quantified spectrophotometrically, and the quality was assessed using agarose gel electrophoresis to verify the presence of two ribosomal RNA bands.

cDNA was synthesized from 5 μg of total RNA isolated from the above tissues using oligo(dT_{18}) primer and RevertAid H Minus M-MuLV reverse transcriptase following the manufacturers instructions (MBI Fermentas, Burlington, ON, Canada). Partial PDK isoform sequences were obtained using degenerate primers (PDK forward and reverse; Table 1) determined from conserved regions of available sequences in GenBank. Primers were designed with the assistance of GeneTool Lite software (version 1.0; DoubleTwist, Oakland, CA; http://www.biotool.com). PCRs were carried out in a PTC-200 MJ Research thermocycler using *Taq* DNA polymerase (MBI Fermentas), and cDNA was isolated from the above tissues. Each PCR reaction consisted of an initial treatment of 5 min at 94°C, followed by 40 cycles of 30 s at 94°C, 30 s at 49°C, and 90 s at 72°C. The resulting PCR products were electrophoresed along with a DNA ladder on 1.5% agarose gels containing ethidium bromide to confirm the presence of a product of the appropriate size (~900 bp). The PCR reactions yielded a single visible band during electrophoresis; therefore, the PCR product was directly ligated into pGEM-T easy vectors (Promega; Fisher Scientific, Nepean, ON, Canada) without gel purification. The ligated product was introduced into heat shock competent *Escherichia coli* (strain 109; Promega) and colonies grown on Luria Bertani agar plates containing 100 ng/ml ampicillin, 0.1 mM isopropyl β-D-1-thiogalactopyranoside, and 20 ng/ml 5-bromo-4-chloro-3-indolyl-b-D-galactoside (X-Cal). Several colonies containing ligated PCR products were selected and grown overnight in liquid culture. Plasmids were harvested from liquid culture using GenElute Plasmid Miniprep kit (Sigma-Aldrich, Oakville, ON, Canada) and sequenced using an ABI377 automated fluorescent sequencer (Applied Biosystems).

Table 1. *PCR primers used for the identification and quantification of PDK mRNA from killifish tissues*

Name	Purpose	Direction	Sequence
PDK	Degenerate	Forward	5′ ccg tc(g/c) cc(g/a) (c/t)tI tc(c/t) at(g/c) 3′
PDK	Degenerate	Reverse	5′ ta(a/c) cca aaI cca gcc a(a/g)I g 3′
PDKFh-2	5′ RACE	Outer primer	5′ tcc ccc gag aga cac cat gac ttt 3′
PDKFh-2	5′ RACE	Inner primer	5′ cca gat cgg gag agc gca ggt aat 3′
PDKFh-2	3′ RACE	Outer primer	5′ gct gct cac tac ccc ctc tgt tca 3′
PDKFh-2	3′ RACE	Inner primer	5′ ggc gca ggg ggt cat aga ata caa 3′
PDKFh-4	5′ RACE	Outer primer	5′ tgg gct cgt ctc gtg cgt ctc ta 3′
PDKFh-4	5′ RACE	Inner primer	5′ acg ccg aac gcc tcc ttg aac t 3′
PDKFh-4	3′ RACE	Outer primer	5′ ggc cag ccc atc cac atc gtt tat 3′
PDKFh-4	3′ RACE	Inner primer	5′ gcc atg cga gcc acc gta gag a 3′
PDKFh-2	qPCR	Forward	5′ ccc acg aga gca gca aca a 3′
PDKFh-2	qPCR	Reverse	5′ ctc ccc cga gag aca cca t 3′
PDKFh-4	qPCR	Forward	5′ agt ccc ctt gag gaa gat cga 3′
PDKFh-4	qPCR	Reverse	5′ gac tcg gag ccg tgg tgt ac 3′
LDHFh-A	qPCR	Forward	5′ acc tat ctt tga gtg gct tta act aca a 3′
LDHFh-A	qPCR	Reverse	5′ atc ata aac ggc aaa gtg 3′
LDHFh-B	qPCR	Forward	5′ agt cca act gcg gtg ttc ct 3′
LDHFh-B	qPCR	Reverse	5′ tgg cct cat act cg 3′

PDK, pyruvate dehydrogenase kinase; RACE, rapid amplification of cDNA ends; qPCR, quantitative PCR; LDH, lactate dehydrogenase.

To obtain complete cDNA sequences, isoform-specific primers were designed to obtain the central fragment of the gene (Table 1), and 3′ and 5′ rapid amplification of cDNA ends (RACE) was performed using a commercial kit [RNA ligase-mediated (RLM)-RACE; Ambion, Austin, Texas] to obtain the remainder of the sequence. Multiple clones of each fragment were sequenced in both directions and a majority-rule consensus for the full-length cDNA transcript was developed for each isoform. Sequence assembly and analysis were performed using GeneTool Lite software. Comparisons with published sequences were made using the BLAST algorithm (1), and multiple alignments were produced with ClustalW (53) to verify gene identity. All full-length sequences have been deposited into GenBank (PDK_{Fh}-2, Bankit 1073889; PDK_{Fh}-4, Bankit 1073891).

Phylogenetic Analysis

Amino acid sequences were deduced from the nucleotide sequence of each isoform using GeneTool Lite software. Protein sequences or deduced amino acid sequences of other PDK genes were obtained from GenBank or genome sequences available on Ensembl: human2 (*Homo sapiens,* NP002602); dog2 (*Canis familiaris,* XP548195); mouse2 (*Mus musculus,* AAH21764); rat2 (*Rattus norvegicus,* NP110499); opossum2 (*Monodelphis domestica,* XP001374336); chimpanzee2 (*Pan troglodytes,* XP001168889); frog2 (*Xenopus leavis,* NP001080097); frog4 (NP001006803); zebrafish3 (*Danio rerio,* XP00133259); zebrafish2 (NP957290); pufferfish (*Tetraodon nigroviridis,* CAF91901); rat1 (NP446278); chicken1 (*Gallus gallus,* NP001026523); mouse1 (NP766253); human1 (NP002601); cow (*Bos Taurus,* XP607085); chicken3 (NP001006259); mouse3 (NP663605); opossum3 (XP001362369); horse (*Equus caballus,* XP001493781); mouse4 (NP038771); dog3 (XP859771); human3 (NP005382); rat4 (NP446003); dog4 (XP539427); human4 (NP002603); chimpanzee 4 (XP527822); monkey4 (*Macaca mulatta*, XP001093255); platypus (*Ornithorhynchus anatinus*, XP001514685); dog1 (XP534032); horse (XP001495143); opossum1 (XP001377950); chimpanzee1 (XP001146941); cow (XP583960); monkey1 (XP001086316); bat4 (*Rhinolophus ferrumequinum*, DQ468386); squirrel4 (*Spermophilus tridecemlineatus*, AF020845); bee (*Apis mellifera*, XP393904); Stickleback2a (*Gasterosteus aculeatus*, Ensemble Gene ID ENSGACG00000003817); Stickleback2 (Ensemble Gene ID ENSGACG00000005722); stickleback4 (Ensemble Gene ID ENSGACG00000006683); stickleback1 (Ensemble Gene ID ENSGACG00000004843); stickleback3 (Ensemble Gene ID ENSGACG00000002603); fugu4 (*Takifugu rubripes*, Ensemble Gene ID ENSTRUG00000015972); fugu2 (Ensemble Gene ID ENSTRUG00000013086).

Phylogenetic analysis was performed using the neighbor-joining methods (41) with complete deletion of gaps using MEGA4 software (51). The support for each node was assessed using 500 bootstrap replicates. Isoforms were named according to their position in the phylogenetic tree.

PDK Isoform Tissues Distribution

Tissue distribution of the two identified killifish PDK isoforms was estimated using quantative PCR (qPCR) with isoform-specific primers. Primers were designed with the assistance of Primer Express software (primer sequences in Table 1; version 2.0.0; Applied Biosystems, Foster City, CA). The same cDNA samples used above for gene identification were used to determine the tissue distribution of each mRNA. qPCR was performed on an ABI 7000 sequence analyzer (Applied Biosytems) using the protocols outlined in Richards et al. (39). The absolute mRNA levels of each PDK isoform among tissues was estimated according to the formula, efficiency^{-Ct}, where efficiency is the slope of a standard curve and Ct corresponds to the threshold cycle number. All results were standardized to total RNA and normalized to the levels of PDK_{Fh}-2 mRNA detected in the brain.

Experimental Protocols

Whole animal respirometry (P_{crit} and $\dot{M}_{O2}$). Routine oxygen consumption rate ($\dot{M}_{O2}$) and critical oxygen tension P_{O_2} (P_{crit}) were determined on individual fish by using closed respirometry. Briefly,

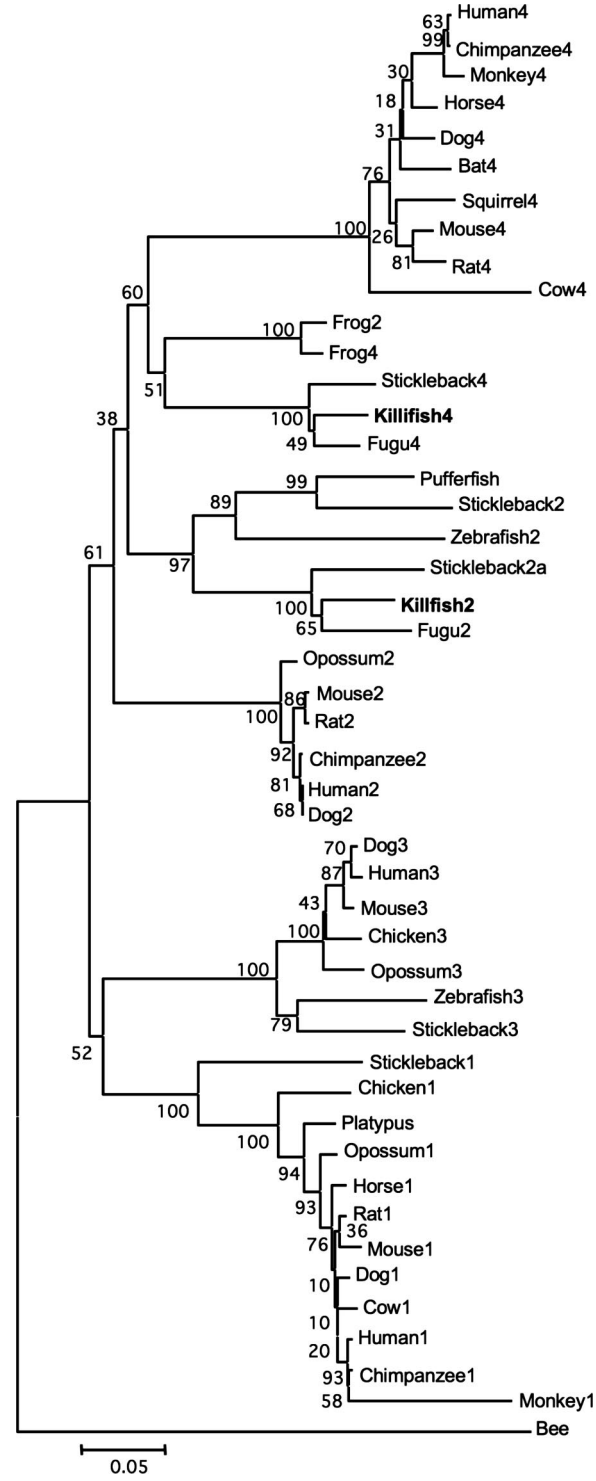

Fig. 1. Phylogenetic analysis of pyruvate dehydrogenase kinase (PDK) isoform amino acid sequences. Numbers presented at each branch point represent bootstrap values from 500 replicates. Boldfaced type indicates PDK isoforms identified in this study, and they have been named according to their position in the phylogenetic tree. Bee PDK was used as an outgroup.

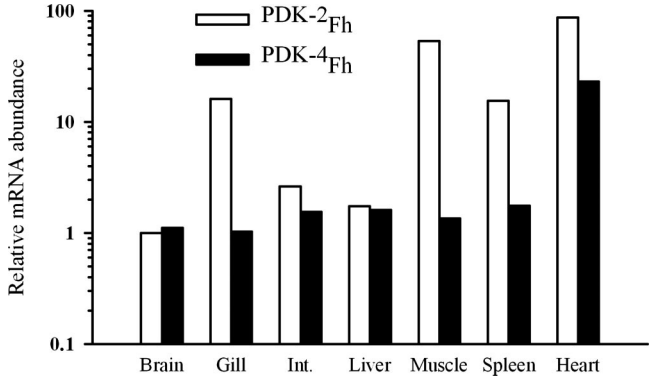

Fig. 2. Relative tissue distribution of PDH kinase isoforms 2 and 4 (PDK_{Fh}-2 and -4) mRNA in brain, gill, intestine (Int), liver, muscle, spleen, and heart. mRNA levels are expressed relative to total RNA and normalized to *PDK_{Fh}-2* levels in the brain, which are set to 1.

individual fish were placed into 250-ml darkened glass respirometers and allowed to habituate for at least 12 h before respirometry. During this period, air-saturated brackish water (10 g/l) was circulated through the respirometer. At the beginning of a trial, water circulation was stopped, an oxygen probe was fixed into each respirometer, and the respirometer was sealed. Water temperature was maintained at 20°C by placing the respirometers in a temperature-regulated wet table. Continuous oxygen readings were obtained using a fiber optic oxygen probe (Foxy system; Ocean Optics, Dunedin, FL), while the water in the respirometer was continuously stirred in one corner with a magnetic stir bar. Oxygen partial pressure was monitored continuously until it decreased $<$ 20 Torr or the fish showed signs of distress. Each trial took ~1.5 h to complete, and the fish typically remained quiescent throughout. Any fish that struggled was removed from the data set. Water oxygen content was corrected for differential solubility in brackish water at 19°C by using solubility coefficients from Boutilier et al. (5) and $\dot{M}_{O2}$ was calculated over sequential 10-min periods using the slope of the oxygen trace (water O_2 over time) corrected for fish weight and respirometer volume. Changes in $\dot{M}_{O2}$ were plotted against the mean water P_{O_2} for each 10-min interval, and the inflection point at which $\dot{M}_{O2}$ transitioned from being dependent on environmental P_{O_2}, termed P_{crit} (36), was determined using the BASIC program designed by Yeager and Ultsch (58).

To understand the temporal effects of hypoxia exposure on $\dot{M}_{O2}$, we measured $\dot{M}_{O2}$ on a separate group of fish over a 30-min period in normoxic water (124 Torr) and after 3-h exposure to 10 Torr. Briefly, fish were introduced to the same respirometers used for the P_{crit} determination and were allowed to habituate overnight. To record resting $\dot{M}_{O2}$ under normoxic conditions, we stopped water flow to the respirometer and monitored water P_{O_2} over ~30 min or to the point at which water P_{O_2} had decreased by 20%, whichever came first. At this point, water flow through the respirometer was reestablished, and the head tank supplying each respirometer was bubbled with nitrogen gas to achieve the desired level of hypoxia (10 Torr). Fish were maintained under these hypoxic flow-through conditions for 2 h 45 min at which point the respirometers were sealed, and $\dot{M}_{O2}$ was determined over a 30-min period.

Hypoxic Exposure for Metabolic Analysis

One day before experimentation, four fish were transferred into each of 14, 4-l plastic exposure chambers that had a mesh-covered top and mesh sides with a 1.2-l reservoir when the exposure chamber was emerged. The exposure chambers containing fish were placed into a 550-l glass aquaria with aeration, and filtered brackish water and maintained at 19°C. Water was circulated from the bulk tank into each chamber via a submersible pump to ensure a uniform oxygen tension throughout the exposure system. Fish were not fed during the 1-day transfer recovery period or during experimentation.

Following the 1-day recovery period, blood, white muscle, and liver were sampled from fish exposed to the normoxic water (127 ± 6 Torr; n = 8). To sample fish, the exposure chamber was gently removed from the aquaria, confining the fish to the bottom 1.2-l reservoir of the chamber. Fish were then anesthetized by injecting a concentrated solution of benzocaine dissolved in 95% ethanol (Sigma-Aldrich; final concentration 1 g/l) into the water. At complete anesthesia ($<$45 s) fish were removed from the water, and a section of trunk musculature was taken posterior to the visceral cavity and immediately freeze-clamped between two aluminum blocks cooled in liquid nitrogen. The liver was also dissected free of the animal and frozen in liquid nitrogen. Tissue sampling from all four fish took $<$2 min and two exposure chambers were sampled for a total of eight fish per sampling time.

Following normoxia sampling, hypoxia was induced by bubbling nitrogen into the large tank of water and covering the surface with plastic. Water P_{O_2} decreased from normoxia to 23 ± 1 Torr over the first 1 h of nitrogen bubbling and was then maintained at 6 ± 1 Torr from 1.5 to 15 h. Water oxygen was monitored inside the exposure chambers using an YSI-85 dissolved oxygen meter. Eight fish were sampled at 3-, 6-, 9-, 12-, and 15-h exposure to hypoxia, as described above. Following the sampling at 15 h, nitrogen gas was replaced with air, and the fish were allowed to recover for 12 h in normoxia (107 ± 5.4 Torr; n = 6) and were then sampled.

Analytical Techniques

Frozen muscle was broken into pieces (50–100 mg) using an insulated mortar and pestle cooled in liquid nitrogen. Several aliquots of muscle were stored separately in liquid nitrogen for determination of the activity of the PDHa as previously described by Richards et al. (38). A portion of the frozen muscle (~50 mg) was ground into a fine

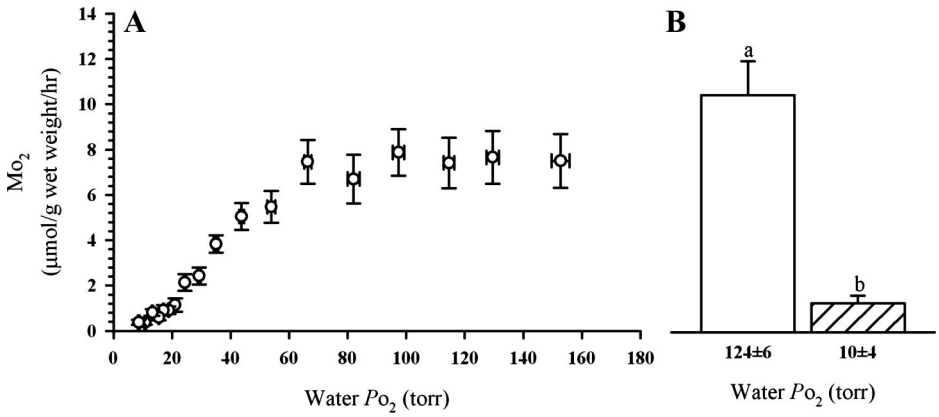

Fig. 3. Oxygen consumption rate ($\dot{M}_{O2}$) of killifish during progressive decreases in environmental P_{O_2} (*A*) and in response to normoxia (open bar in *B*) and 3-h hypoxia exposure (hatched bar in *B*). *A* and *B* share the same *y*-axis. Date are means ± SE (n = 8). Bars with different letters in *B* are significantly different.

powder under liquid nitrogen and used for intracellular pH (pH_i) measurements as described by Pörtner et al. (35). The remaining muscle was lyophilized for 72 h, dissected free of connective tissue, powdered, and stored dry at −80°C for subsequent analysis.

For the determination of muscle glycogen, ~20 mg of lyophilized muscle was digested in 1 ml 30% KOH at 100°C. Glycogen was isolated as described by Hassid and Abraham (17), and free glucose was determined after digestion with amyloglucosidase (2). For the extraction of metabolites from white muscle, aliquots of lyophilized muscle (~20 mg) were weighed into borosilicate tubes, 1 ml of ice-cold 1 M $HClO_4$ was added, and then homogenized at the highest speed of a Syngene homogenizer for 20 s at 0°C. Homogenates were transferred to 2-ml microcentrifuge tubes, centrifuged at 4°C for 5 min at 20,000 *g*, and the supernatant was neutralized with 3 M K_2CO_3, except for samples for ammonia analysis, which were neutralized with 3M Tris-base. Neutralized extracts were assayed spectrophotometrically for ATP, CrP, creatine, lactate, pyruvate, glutamate, α-ketoglutarate, and glucose using the spectrophotometric methods described in Bergmeyer (2). Muscle ammonia was analyzed using a commercial kit (Sigma). Muscle acetyl-CoA was determined on neutralized extracts by radiometric methods previously described in Richards et al. (38).

The expression patterns of killifish PDK mRNA were estimated using qPCR and the isoform-specific primers used above and given in Table 1. The expression pattern of lactate dehydrogenase LDH-A (muscle) and LDH-B (liver) mRNA were examined using qRT-PCR primers (Table 1) designed from LDH-A and -B sequences from GenBank (LDH-A accession no. L43525; LDH-B accession no. M33969). Briefly, total RNA was extracted from ~20 mg of muscle or liver and 5 μg of total RNA was reverse transcribed into cDNA using the protocols outlined above. qPCR was performed as described in Richards et al. (39). qPCR reactions contained 2 μl of cDNA, 4 pmol of each primer, and Universal SYBR Green master mix (Applied Biosystems) in a total volume of 20 μl. All qPCR reactions were performed as follows: 2 min at 50°C, 10 min at 95°C, followed by 40 cycles of 95°C for 15 s and 60°C for 1 min. Melt curve analysis was performed following each reaction to confirm the presence of only a single product of the reaction. To control for genomic contamination, negative control samples were performed using RNA that had not be reversed transcribed. Genomic DNA contamination was present for all genes examined, but never constituted more than 1:1024 copies (<0.1%) for any gene. One randomly selected control sample was used to develop a standard curve relating threshold cycle to cDNA amount for each primer set. All results were expressed relative to these standard curves, and mRNA amounts were normalized to the expression of elongation factor (EF-1α), which was measured using primers described by Scott et al. (42). There was no effect of hypoxia exposure on the expression of EF-1α when expressed as a function of total RNA (data not shown); thus EF-1α appears to be a good control gene for hypoxia studies. Expression levels in hypoxia-exposed animals were expressed relative to the mean expression levels in the normoxia control samples. All samples were run in duplicate and the coefficient of variation between duplicate samples was always <15%.

PDH kinase 2 protein content was assessed using immunoblot analysis according to the protocols described in Richards et al. (40). Briefly, muscle samples (~20 mg) were homogenized in a buffer containing 100 mM TRIS·HCl, 1% SDS, 5 mM EDTA, 1 μg/ml aprotinin, 1 μg/ml pepstatin A, 1 μg/ml leupeptin, and 20 μg/ml PMSF, pH 7.5. Homogenates were centrifuged at 5,000 *g* for 10 min at 4°C, the supernatant was assayed for total protein using the methods of Bradford (7), and a portion of the supernatant was denatured by boiling for 3 min in SDS-sample buffer (26). Denaturing SDS-polyacrylamide gels were loaded with denatured muscle homogenates at a protein concentration of 20 μg protein/lane, and electrophoresed for 15 min at 75 V followed by 75 min at 150 V. An identical control sample was included on each gel to control for gel-to-gel variation. Following the electrophoresis, proteins were transferred to nitrocellulose membranes (Bio-Rad Laboratories) using a Trans-Blot semidry transfer cell (Bio-Rad). Blots were incubated for 1 h with 1 μg/ml of primary antibody (raised against the COOH-terminal end of rabbit PDK-2; peptide sequence 5′-VPSTEPKNTSTYRVS-′3; Abgent, San Diego, CA) and then subsequently incubated for 1 h with alkaline phosphatase-conjugated goat-anti-rabbit IgG secondary antibody (Stressgen, Ann Arbor, MI). Immunoblots were developed in alkaline phosphatase buffer containing 5-bromo-4-chloro-3-indolylphosphate and nitroblue tetrazolium, and the band intensity was quantified using a FluorChem 8800 image analyzer (Alpha Innotech, San Leandro, CA) and AlphaEase FC software (version

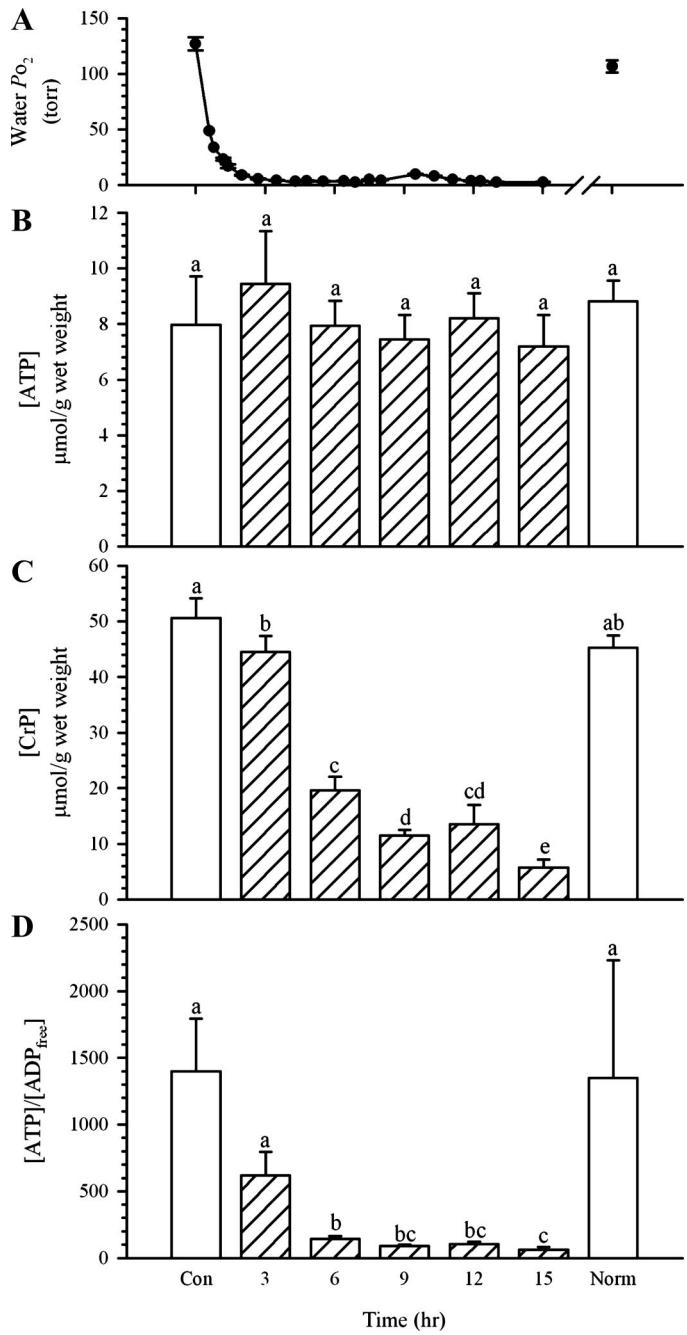

Fig. 4. Water P_{O_2} (*A*), white muscle [ATP] (*B*), [CrP] (*C*), and [ATP]/[ADP_{free}] (*D*) during normoxia, up to 15-h exposure to hypoxia, and after 12-h recovery in normoxia. Data are means ± SE ($n = 6–8$). Values with different letters are significantly different ($P < 0.05$).

3.1.2). Individual samples were expressed relative to total protein, and subsequently each sample was normalized to the mean of the normoxia control samples.

Calculations and Statistical Analysis

Free cytosolic [ADP] and [AMP] were calculated from measured values of [ATP], [CrP], [creatine] ([Cr]), and pH_i according to published protocols (13, 52), assuming equilibrium of the creatine kinase (K'_{CK}) and adenylate kinase (K'_{AK}) reactions. The equilibrium constants for K'_{CK} and K'_{AK} were corrected for experimental temperature, pH, and free Mg^{2+} (assumed to be 1 mM; see Refs. 13 and 52). Cellular phosphorylation potential was calculated according to the following equation

$$\frac{[ATP]}{[ADP][P_i]} = \frac{[CrP]K'_{CK}}{[Cr][P_i]}$$

Cytosolic free $[P_i]$ was estimated assuming the inverse of CrP hydrolysis and starting with a resting tissue level of 1 μmol/g wet weight (16). The Gibbs free energy of ATP hydrolysis ($\Delta_f G'$; kJ/mol) was determined using the following equation

$$\Delta_f G' = \Delta_f G'^{\circ}_{ATP} + R\mathrm{T}\ln\frac{[ADP_{free}][P_i]}{[ATP]}$$

where R is the universal gas constant (8.3145 $J \cdot K^{-1} \cdot mol^{-1}$), T is temperature in K, and $\Delta_f G'^{0}_{ATP}$ is the standard transformed Gibbs energy of ATP hydrolysis ($\Delta_f G'^{0}_{ATP} = -R\mathrm{T}\ln K'_{ATP}$) at measured pH and temperature and estimated free $[Mg^{2+}]$. Cytoplasmic $[NAD^+]$/[NADH] was estimated using the apparent equilibrium of the lactate dehydrogenase reaction [Keq from Wang et al., (55)] and measured pH_i, [lactate], and [pyruvate]. Mitochondrial $[NAD^+]$/[NADH] was estimated from the glutamate dehydrogenase (GDH) reaction using whole cell measurements of $[NH_3]$, [glutamate], [α-ketoglutarate], K_{eq} from Williamson et al. (57) and estimated mitochondrial pH from Moyes et al. (31). All data are presented as means ± SE (n). All metabolite concentrations determined on lyophilized tissues were converted back to wet weights by taking into account a wet-to-dry ratio of 4:1 (55). Statistical analysis consisted of a one-way ANOVA followed by the Holm-Sidak post hoc method of pairwise multiple comparisons. All data were tested for normality (Kolmogorov-Smirnov test) and homogeneity of variance (Levene median test), and in cases where data sets did not meet these assumptions, data were log transformed and statistical analyses were repeated. For a small number of cases where log transformation did not yield data of normal distributed or equal variance, Kruskal Wallis one-way ANOVA on ranks was used for statistical analysis. Results were considered significant at $P < 0.05$.

RESULTS

PDH Kinase Isoforms in Killifish

Two full-length cDNA sequences coding for PDK were identified in killifish. Alignment of these killifish isoforms with other vertebrate PDK isoforms indicated that our killifish isoforms were 52–75% similar to other known fish and mammalian PDK isoforms. Phylogenetic analysis of the deduced amino acid sequence of these two killifish isoforms indicated that one isoform grouped more closely with other known PDK-4 isoforms (designated PDK_{Fh}-4), and the other isoform grouped closely with other known PDK-2 isoforms (designated PDK_{Fh}-2; Fig. 1). No isoforms matching PDK-1 or -3 were detected. PDK_{Fh}-2 and PDK_{Fh}-4 cDNA sequences have coding regions of 1224 and 1230 nucleotides, yielding an open reading frame of 409 and 410 amino acids, respectively.

In all tissues except brain, *PDK_{Fh}-2* was expressed at higher levels than *PDK_{Fh}-4* when examined relative to total tissue RNA (Fig. 2). Highest expression of *PDK_{Fh}-2* was observed in heart, muscle, gill, and spleen, and *PDK_{Fh}-4* was only highly expressed in the heart, with barely detectable levels of PDK_{Fh}-*4* mRNA in all other tissues. When tissue distributions were expressed relative to the levels of the control gene EF-1α (data not shown), the tissue distribution patterns of *PDK_{Fh}-2* and *-4* were qualitatively similar to that observed when normalized to total RNA.

Responses of Killifish to Hypoxia

Oxygen consumption rate and P_{crit}. During progressive decreases in environmental P_{O_2}, $\dot{M}_{O_2}$ remained constant from water P_{O_2} levels of 153 ± 3 Torr to 66 ± 1 Torr, below which $\dot{M}_{O_2}$ decreased in a near-linear fashion with environmental P_{O_2} (Fig. 3*A*). The point at which killifish transition their $\dot{M}_{O_2}$ from being independent of environmental P_{O_2} to being dependent on environmental P_{O_2} was 63.9 ± 5.6 Torr ($n = 6$). Killifish exposed to hypoxia for 3 h (water P_{O_2} 10 ± 4 Torr) and tested under hypoxia had approximately sevenfold lower $\dot{M}_{O_2}$ than killifish exposed to normoxic water (water P_{O_2} 124 ± 6 Torr; Fig. 3*B*).

Hypoxia Exposure

Water oxygen decreased over the first 1.5-h exposure from normoxia (127 ± 6 Torr; $n = 8$) to hypoxia and then

Table 2. *White muscle free creatine, pHi, ADP_{free}, AMP_{free}, ATP/AMP_{free}, phosphorylation potential, and $\Delta_f G'$ in killifish exposed to normoxia (127 ± 6 Torr, n = 8), ≤ 15-h hypoxia (6 ± 1 Torr; n = 131), and after 12-h recovery in normoxia*

	Time						
Measure	Normoxia	3 h	6 h	9 h	12 h	15 h	Recovery
Creatine	9.2±4.4[a]	22.8±7.3[a]	41.5±2.5[b]	54.6±4.0[b]	54.9±10.3[b]	56.6±8.4[b]	22.5±5.7[a]
pHi	7.26±0.03[a]	7.15±0.04[b]	7.03±0.03[c]	6.86±0.02[d]	6.87±0.04[d]	6.78±0.03[d]	7.25±0.02[a]
ADP_{free}	12.3±4.5[a]	21.8±7.7[ab]	59.6±8.1[bc]	89.1±14.3[d]	91.1±20.6[d]	157.5±30.1[c]	24.1±7.4[b]
AMP_{free}	0.03±0.01[a]	0.08±0.03[a]	0.62±0.17[a]	1.35±0.32[a]	1.34±0.52[a]	5.30±1.81[b]	0.14±0.06[a]
ATP/AMP_{free}, 10^{-3}	2335±982[a]	448±221[b]	19±4[b]	7±1[b]	10±3[b]	6±4[b]	807±545[ab]
Phos Potent, 10^{-3}	1555±507[a]	554±153[b]	60±13[b]	21±4[b]	31±10[b]	10±6[b]	1242±816[a]
$\Delta_f G'$	−66.8±0.9[a]	−64.0±0.7[ab]	−55.1±0.5[b]	−54.8±0.4[bc]	−55.3±1.0[bc]	−50.9±1.1[c]	−65.5±1.7[a]

Data are means ± SE ($n = 6–8$). pH_i, intracellular pH; ADP_{free}, free ADP; AMP_{free}, free AMP; Phos Potent, phosphorylation potential; $\Delta_f G'$, Gibbs free energy of ATP hydrolysis. Cr is reported in μmol/g wet tissue, ADP_{free} and AMP_{free} are reported in nmol/g wet tissue, and $\Delta_f G'$ is reported in kJ/mol. Values with different letters are significantly different ($P < 0.05$).

stabilized at 6 ± 1 Torr (n = 131) for the 15-h duration of the hypoxia exposure (Fig. 4*A*). During the decline in environmental oxygen, there was an initial period where the fish appeared agitated and were observed swimming around the top of each chamber, but by 2 h after the initiation of hypoxia, all fish were quiescent at the bottom of their individual chambers and remained in this state throughout the hypoxia exposure. Killifish that experienced 15-h exposure to hypoxia followed by 12-h recovery in normoxic water remained quiescent throughout the hypoxia and recovery period. No mortality was observed as a result of the hypoxia exposure or recovery.

Metabolic Responses in Muscle

White muscle [ATP] was not affected by exposure to hypoxia or hypoxia followed by 12-h recovery in normoxic water (recovery group; Fig. 4*B*). Exposure to hypoxia caused an initial 13% decrease in white muscle [CrP] over the first 3 h, which continued to decrease to 11% of the normoxic [CrP] values at 15-h exposure to hypoxia (Fig. 4*C*). White muscle [CrP] in the recovery group was similar to that observed in the initial normoxic control. Changes in white muscle free [Cr] were reciprocal and roughly stiochiometric to the changes observed in white muscle [CrP] (Table 2). White muscle pH_i decreased within the first 3-h exposure to hypoxia and continued to decrease until 9 h, where white muscle pH_i stabilized at ~6.8 until 15 h (Table 2). pH_i was similar between the initial normoxic controls and in the recovery group. Estimated [ADP_{free}] and [AMP_{free}] both increased in response to hypoxia exposure, although [ADP_{free}] was elevated by 6-h exposure to hypoxia, whereas [AMP_{free}] was only elevated after 15-h exposure to hypoxia (Table 2). Muscle [AMP_{free}] returned to normoxic levels in the recovery group, while [ADP_{free}] remained elevated compared with the normoxic controls. As a result of these changes in free adenylates, cellular energy charge ([ATP]/[ADP_{free}]) and [ATP]/[AMP_{free}] were significantly depressed after 6- and 3-h exposure to hypoxia, respectively, and remained low for the full 15-h exposure to hypoxia (Fig. 4*D* and Table 2). In the recovery group, both [ATP]/[ADP_{free}] and [ATP]/[AMP_{free}] were similar to the normoxic control values. Muscle phosphorylation potential was significantly depressed by 3-h exposure to hypoxia and continued to decrease throughout the hypoxia exposure returning to values that were not significantly different from the normoxic controls in the recovery group (Table 2). The $\Delta fG'$ decreased significantly by 6-h exposure to hypoxia and continued to decline until 15-h hypoxia exposure (Table 2). In the recovery group, $\Delta fG'$ was not different from that observed in the normoxic controls.

White muscle [glycogen] was variable in normoxia-exposed killifish, but showed a decreasing trend in response to 15-h exposure to hypoxia, returning to values that were similar to the initial normoxic controls in the recovery group (Fig. 5*A*). White muscle [glucose] did not change over the first 3-h exposure to hypoxia, but increased significantly thereafter, returning to levels equivalent to the initial normoxic control in the recovery group (Table 3). Lactate accumulated in a nearly linear fashion over the first 9-h exposure to hypoxia and then stabilized and accumulated at a slower rate (Fig. 5*B*). A complete recovery of white muscle [lactate] was observed in the recovery group. Exposure to hypoxia or recovery did not significantly affect white muscle [pyruvate] (Table 3). White muscle [acetyl-CoA] increased 1.2-fold over the first 3-h exposure to hypoxia and remained elevated for the full 15-h exposure to hypoxia, only returning to normoxic values in the recovery group (Table 3). Muscle cytoplasmic redox state ([NAD^+]/[NADH]) estimated from changes in lactate, pyruvate, and pH_i decreased rapidly and significantly over the first 3-h exposure to hypoxia and remained low for the full 15-h exposure (Fig. 5*C*). Some recovery of cytoplasmic redox was observed in the recovery group, but [NAD^+]/[NADH] remained reduced compared with the initial normoxic control.

White muscle [NH_3] increased over the 15-h exposure to hypoxia, while muscle glutamate decreased over the same period (Table 4). Hypoxia exposure did not affect white muscle α-ketoglutarate (Table 4). Estimated mitochondrial [NAD^+]/[NADH] did not change significantly in response to hypoxia

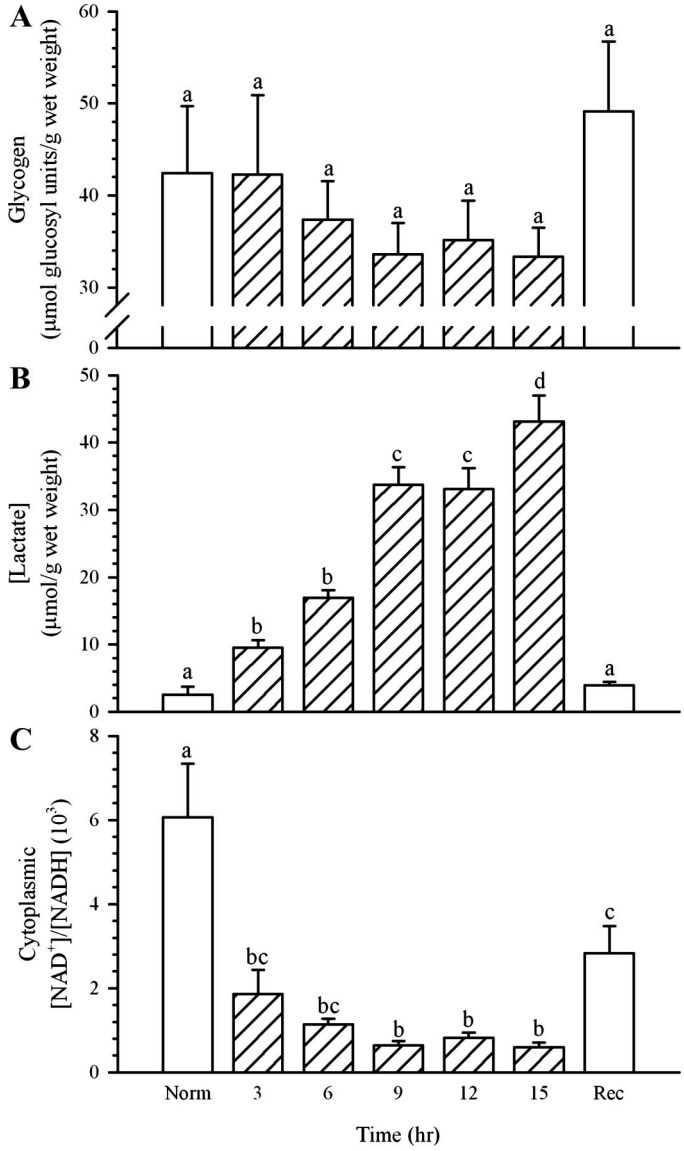

Fig. 5. White muscle [glycogen] (*A*), [lactate] (*B*), and cytoplasmic [NAD^+]/[NADH] (*C*) in killifish exposed to normoxia (127 ± 6 Torr, n = 8), up to 15-h hypoxia (6 ± 1 Torr, n = 131), and after 12-h recovery in normoxia. Data are means ± SE (n = 6–8). Values with different letters are significantly different ($P < 0.05$).

Table 3. *White muscle glucose, pyruvate, acetyl-CoA concentrations, and LDH-A mRNA in killifish exposed to normoxia (127 ± 6 Torr, n = 8), ≤ 15-h hypoxia (6 ± 1 Torr, n = 131), and after 12-h recovery in normoxia*

	Time						
Measure	Normoxia	3 h	6 h	9 h	12 h	15 h	Recovery
Glucose	1.23±0.11[a]	1.37±0.12[a]	1.87±0.05[b]	2.45±0.19[c]	2.65±0.07[cd]	2.92±0.19[d]	1.46±0.08[a]
Pyruvate	0.26±0.03[a]	0.42±0.04[a]	0.42±0.07[a]	0.33±0.04[a]	0.41±0.04[a]	0.31±0.05[a]	0.35±0.05[a]
Acetyl-CoA	0.90±0.10[a]	1.16±0.07[bc]	1.11±0.12[abc]	1.33±0.07[b]	1.35±0.08[b]	1.39±0.10[b]	0.98±0.04[c]
LDH-A mRNA	1.00±0.09[a]	0.93±0.21[a]	0.93±0.14[a]	1.12±0.22[a]	0.85±0.13[a]	1.09±0.34[a]	1.31±0.19[a]

Data are means ± SE (n = 6–8). Glucose and pyruvate are reported in μmol/g wet tissue; acetyl-CoA is reported in nmol/g wet tissue; and *LDH-A* mRNA is reported relative to the expression of a control gene, elongation factor (EF)-1α. Values with different letters are significantly different ($P < 0.05$).

exposure or recovery, but there was an overall trend for a higher [NAD^+]/[NADH] during hypoxia exposure compared with normoxic controls or recovery.

The activity of PDHa decreased by ~50% within 3-h exposure to hypoxia and remained at this low level for the full 15-h exposure, returning to values that were not significantly different from those in the recovery group (Fig. 7*A*). Total PDK-2 protein showed a general decrease of nearly 40%, between 6 and 15 h of hypoxia exposure (Fig. 7*B*). A full recovery of PDK-2 protein was observed in the recovery group. PDK_{Fh}-*2* mRNA in white muscle increased ~3.8-fold over the first 9-h exposure to hypoxia and continued to increase to 10.2 times the normoxic values at 15 h (Fig. 7*C*). In the recovery group, the level of PDK_{Fh}-*2* expression was similar to the initial normoxic values. Exposure to hypoxia had no effect on PDK_{Fh}-*4* mRNA expression in white muscle (Fig. 7*D*). White muscle *LDH-A* mRNA expression did not change in response to hypoxia exposure to recovery (Table 3).

Liver

Hypoxia exposure did not affect the expression pattern of *LDH-B* or PDK_{Fh}-*4* in liver (Table 5). In contrast, liver PDK_{Fh}-*2* expression transiently decreased, by ~38%, over the first 3-h exposure to hypoxia, returned to values that were not significantly different from the controls between 6 and 12 h, and significantly decreased again at 15-h exposure (Table 5). PDK_{Fh}-*2* expression in the recovery group was similar to that observed in the initial normoxic control.

DISCUSSION

Hypoxia survival in killifish was associated with a strong activation of substrate-level phosphorylation coupled with a depression of whole animal $\dot{M}_{O2}$. In killifish muscle, these responses occurred in a biphasic fashion and showed a strong dependence on muscle CrP hydrolysis (Fig. 4*C*) and glycolytic production of lactate (Fig. 5*B*) to support ATP turnover during the first 6-h exposure to hypoxia. This was followed by a period of substantially reduced utilization of CrP and lower lactate accumulation at > 9-h exposure. Fish white muscle is generally considered a "closed" system, with little exchange of metabolites, in particular, lactate, with the extracellular fluid (54); therefore, these data indicate that during the first 6 h of exposure to hypoxia, increases in substrate-level phosphorylation are necessary to make up for the reduced capacity for ATP generation. After the first 6 h of exposure to hypoxia, the smaller changes in muscle metabolite concentrations coincide with stable muscle [ATP] (Fig. 4*B*) and suggest dramatic reductions in ATP consumption and tissue metabolic rate depression.

Although maintenance of a constant cellular [ATP] during hypoxia exposure (Fig. 4*B*) has been termed the "hallmark" of a hypoxia-tolerant animal, there was still a substantial disruption of cellular energetics and a loss of phosphorylation potential (Table 2) during hypoxia exposure. The loss of phosphorylation potential would have dramatic effects on the rates of ATP utilization as well as rates of cellular ATP production and substrate oxidation. In particular, hypoxia exposure was associated with a significant drop in $\Delta_f G'$ from −66.8 kJ/mol to −50.9 kJ/mol over 15 h (Table 2). Estimates of the critical limit of $\Delta_f G'$ for the maintenance of cellular function (16, 21) suggest that below a threshold of −52 kJ/mol, cellular processes such as ion pumping can no longer derive sufficient energy from ATP hydrolysis to be maintained. Thus, although total tissue [ATP] is not affected by hypoxia exposure, significant disruption in cellular energy balance is still observed in response to hypoxia, and this disruption affects rates of cellular ATP use and production.

The control of metabolic rate depression is thought to be primarily regulated by the kinetics of mitochondrial substrate oxidation (4). Consistent with this notion is the rapid (3-h) and

Table 4. *White muscle total ammonia, glutamate, α-ketoglutarate, and estimated mitochondrial [NAD^+]/[NADH] in killifish exposed to normoxia (127 ± 6 Torr, n = 8), ≤ 15-h hypoxia (6 ± 1 Torr, n = 131), and after 12-h recovery in normoxia*

	Time						
Measure	Normoxia	3 h	6 h	9 h	12 h	15 h	Recovery
NH_3	0.23±0.05[a]	0.34±0.07[ab]	0.44±0.09[b]	0.53±0.10[bc]	0.44±0.01[bc]	0.54±0.05[c]	0.29±0.03[ab]
Glutamate	1.88±0.13[a]	1.54±0.15[ab]	1.29±0.08[bc]	1.33±0.17[bc]	1.20±0.13[bc]	1.00±0.12[c]	1.58±0.15[ab]
α-Ketoglutarate	0.41±0.49[a]	2.16±1.13[a]	3.91±1.80[a]	3.66±1.40[a]	0.39±0.54[a]	1.36±1.20[a]	0.91±0.97[a]
Mitochondrial [NAD^+]/[NADH]	0.04±0.01[a]	0.22±0.08[a]	0.35±0.11[a]	0.40±0.15[a]	0.08±0.04[a]	0.29±0.12[a]	0.11±0.08[a]

Data are means ± SE (n = 6–8). Total ammonia (NH_3) and glutamate are reported in μmol/g wet tissue, and α-ketoglutarate is reported in nmol/g wet tissue. Values with different letters are significantly different ($P < 0.05$).

Table 5. *Liver LDH-B, PDK-2, and PDK-4 mRNA in killifish exposed to normoxia (127 ± 6 Torr, n = 8), ≤ 15-h hypoxia (6 ± 1 Torr, n = 131), and after 12-h recovery in normoxia*

	Time						
Measure	Normoxia	3 h	6 h	9 h	12 h	15 h	Recovery
LDH-B	1.00±0.32[a]	1.14±0.19[a]	0.99±0.09[a]	0.86±0.07[a]	1.02±0.11[a]	0.98±0.08[a]	0.90±0.10[a]
PDK_{Fh}*-2*	1.00±0.21[ac]	0.62±0.02[b]	0.72±0.03[bc]	0.74±0.11[bc]	0.82±0.05[a]	0.67±0.06[b]	1.10±0.11[a]
PDK_{Fh}*-4*	1.00±0.13[a]	1.00±0.06[a]	0.72±0.05[a]	0.76±0.05[a]	1.04±0.13[a]	1.02±0.10[a]	0.79±0.06[a]

Data are means ± SE ($n = 6–8$). Gene expression is reported relative to the expression of a control gene (EF-1α). Values with different letters are significantly different ($P < 0.05$).

sustained reduction in muscle PDHa activity during hypoxia exposure (Fig. 6*A*), which limits the rate of mitochondrial pyruvate oxidation, facilitating pyruvate reduction to lactate via cytoplasmic LDH (Fig. 5*B*). The conversion of pyruvate to lactate and the large accumulation of muscle lactate (Fig. 5*B*) during hypoxia exposure is meant to aid in the maintenance of cytoplasmic [NAD^+]/[NADH] for sustained glycolytic flux; however, our estimates of cytoplasmic [NAD^+]/[NADH] indicate that the cytoplasm rapidly becomes reduced during hypoxia exposure (Fig. 5*C*).

Decreases in [NAD^+]/[NADH] and increases in [acetyl-CoA]/[free-CoA] are known to activate PDK, which in turn phosphorylates and inactivates PDH (50). Increases in cellular [pyruvate] and decreases in [ATP]/[ADP_{free}] are permissive to PDH activation via inhibition of PDK. The decrease in muscle PDH activity observed at 3-h exposure to hypoxia was primarily associated with a modest, but significant, increase in muscle [acetyl-CoA] (Table 2) and a lack of increase in cellular [pyruvate] (Table 2) and [ATP]/[ADP_{free}] (Fig. 4*D*). The dramatic and rapid decrease in cytoplasmic [NAD^+]/[NADH] (Fig. 5*C*) did not appear to be communicated to the mitochondrial matrix. In fact, estimates of mitochondrial [NAD^+]/[NADH] using the GDH equilibrium suggest that the mitochondrial matrix was either not affected by hypoxia exposure or became oxidized during hypoxia exposure, which would act to powerfully inhibit PDK and thus facilitate the activation of PDH. These inconsistent cellular signals for the inactivation of PDH via PDK were, however, consistent with isoform-specific regulation as described by Bowker-Kinley et al. (6). Kinetic analysis of recombinant PDK isoforms constructed from rat sequences indicated that PDK-2 is more sensitive to [acetyl-CoA]/[CoA-SH] than [NAD^+]/[NADH], whereas PDK-4 is more sensitive to [NAD^+]/[NADH]. Killifish muscle contains ~40 times more PDK_{Fh}-2 mRNA transcripts than PDK_{Fh}-4, suggesting that PDK_{Fh}-2 is the primary isoform present and therefore regulated to a greater degree by the increase in [acetyl-CoA] (Table 3).

Considerable controversy surrounds the use of the LDH and GDH equilibrium for estimating cytoplasmic and mitochondrial [NAD^+]/[NADH] in tissues (e.g., see Ref. 22). For example, although GDH is restricted to the mitochondrial matrix and is potentially useful for estimating mitochondrial [NAD^+]/[NADH], the total activity of GDH is low, in part due to a low mitochondrial volume density in muscle; and there is uncertainty to what extent cytoplasmic levels of NH_3, glutamate and α-ketoglutarate influence the enzyme equilibrium. The usefulness of the LDH reaction for estimating cytoplasmic [NAD^+]/[NADH] has also been drawn into question because there is evidence that LDH is not isolated to the cytoplasm but is also located in the mitochondrial fraction of fish white muscle (30). It is unlikely, however, that the presence of mitochondrial LDH influences our estimates of cytoplasmic [NAD^+]/[NADH] to a great degree because of the low mitochondrial content characteristic of fish white muscle. Overall, our estimates of cytoplasmic and mitochondrial [NAD^+]/[NADH] in killifish muscle must be considered tentative and await confirmation by other methods.

We observed a rapid inhibition of PDH in killifish muscle during hypoxia exposure that was consistent with work in mammalian ischemic/hypoxia cell models. These studies suggest that modulation of PDHa activity during hypoxia exposure is essential to cell survival leading to a stabilization of cellular [ATP] (43), an attenuation of hypoxia-related ROS generation (24), and inhibition of mitochondrial-induced apoptotic pathways (e.g., see Ref. 12). Important to the inhibition of PDH in mammalian cell culture systems during hypoxia (24) is the HIF-1-mediated increases in the expression of PDK-1 (23, 24). Four PDK isoforms have been identified in mammals (Fig. 1), but our gene identification approach using degenerate primes (Table 1) identified only two isoforms that loosely group with other known PDK-2 and -4 isoforms, each with a specific tissue distribution (Fig. 2). Fish often possess more isoforms than mammals because of genome duplication events (e.g., stickleback have two PDK-2 isoforms; Fig. 1), but our degenerate primers and PCR protocols only amplified a single representative of each of PDK-2 and -4. Of the isoforms identified in killifish, only PDK_{Fh}*-2* was shown to be hypoxia responsive in muscle with mRNA levels increasing > 10-fold during the 15-h hypoxia exposure (Fig. 6*C*). The qRT-PCR primers used to amplify PDK_{Fh}*-2* were designed in a highly variable portion of the gene and therefore can be considered highly gene specific and unlikely to yield amplification of other unidentified PDK-2 isoforms that may be present in the killifish genome. The hypoxia-induced increases in PDK_{Fh}*-2* expression in killifish muscle suggest that this gene could be regulated by HIF via a hypoxic responsive element in the promoter region of PDK_{Fh}*-2*. However, the expression of other genes that are known to have associated hypoxic responsive element (37, 44), including muscle *LDH-A* (Table 3) and liver *LDH-B* (Table 5), were not affected by the hypoxia exposure in killifish, thus bringing into question whether other signal transduction pathways may be involved in regulating the PDK_{Fh}*-2* hypoxic response. Other signal transduction cascades (e.g., MAPK; 27) are known to be activated during hypoxia and could contribute to the regulation of PDK_{Fh}*-2* expression during hypoxia exposure in killifish muscle. Additional work characterizing the transcription factor binding sites in the promoter regions of PDK_{Fh}*-2* is warranted. No changes in

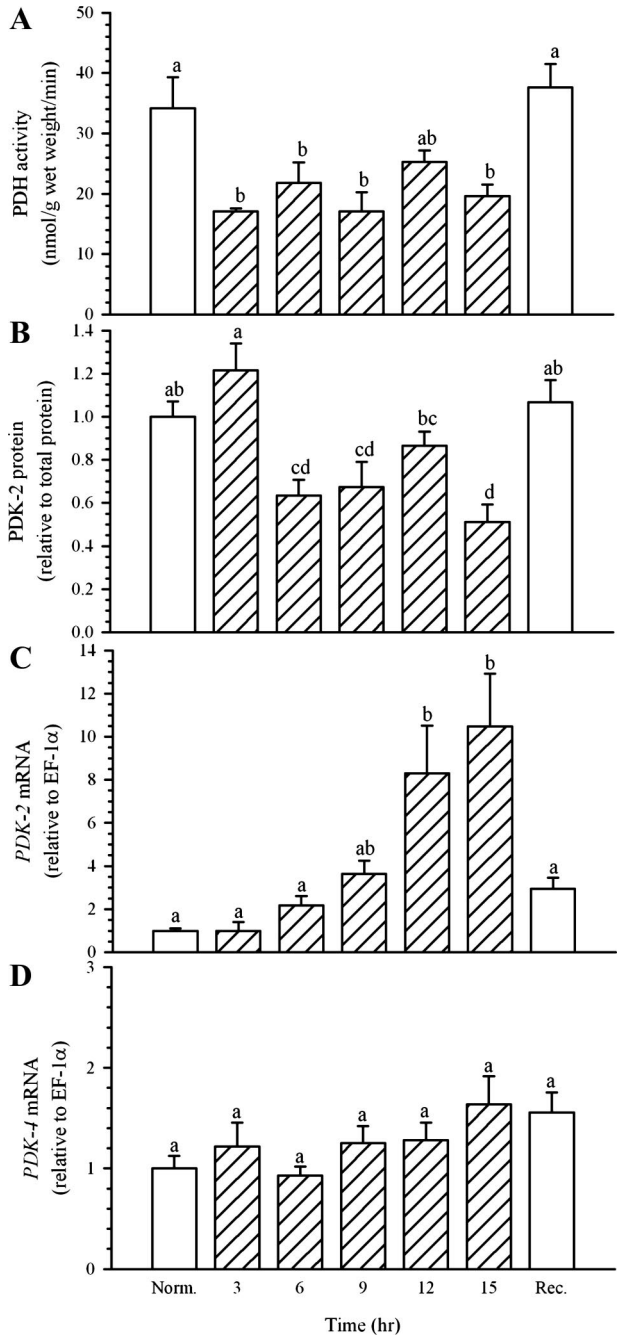

Fig. 6. White muscle protein pyruvate dehydrogenase active form (PDHa) activity (*A*), PDK-2 total protein (*B*), PDK_{Fh}-*2* (*C*), and PDK_{Fh}-*4* (*D*) mRNA in killifish during normoxia, up to 15-h hypoxia exposure, and after 12-h recovery in normoxia. Hypoxia and recovery samples for PDK-2 total protein (*B*) and the expression of PDK_{Fh}-*2* (*C*) and PDK_{Fh}-*4* (*D*) are normalized to the normoxic control sample. EF, elongation factor. Data are means ± SE (n = 6–8). Values with different letters are significantly different ($P < 0.05$).

muscle PDK_{Fh}-*4* mRNA were observed (Fig. 6*D*), but the heart-specific expression pattern of PDK_{Fh}-*4* (Fig. 2) suggests that this isoform may only be important in heart tissues.

In spite of the hypoxia sensitivity of PDK_{Fh}-*2* expression in muscle (Fig. 6*C*), PDK_{Fh}-*2* expression was not hypoxia sensitive in the liver of killifish. In fact, the expression of PDK_{Fh}-*2* significantly decreased within the first 3-h exposure to hypoxia and remained somewhat depressed compared with both the normoxia and recovery sample (Table 3). Similarly, the expression of both PDK_{Fh}-*4* and *LDH-B* in the liver was not affected by the hypoxia exposure (Table 3). Clearly, patterns of gene expression in response to hypoxia exposure are specific to the tissues examined, which is consistent with the tissue-specific enzyme responses observed in the gulf killifish (*F. grandis*) acclimated to moderate hypoxia (~3.6 kPa or 27 Torr) for 1 mo (29). Martinez et al. (29) observed significant increases in the activities of five out of the eleven glycolytic enzymes that were analyzed in the liver (including LDH), which suggests a strong activation of substrate-level phosphorylation and oxygen-independent ATP production. In the same study, the results observed in liver differed dramatically from those observed in muscle where there were clear decreases in glycolytic enzyme activities, suggesting, unlike the liver, the muscle undergoes a substantial metabolic rate depression. Combined, these results suggest that the liver of killifish may make up for the hypoxia-imposed energy deficit through a strong activation of glycolysis, whereas in the muscle, strong inhibition of mitochondrial oxygen consumption and overall tissue metabolic rate depression may play a more important role in insuring hypoxia survival.

There is a lack of association between the hypoxia-induced changes in muscle PDK_{Fh}-*2* mRNA expression and PDK-2 protein content (c.f. Fig. 6, *B* and *C*), such that the changes in mRNA were not translated into increased protein content during hypoxia exposure. Why then are there changes in mRNA transcription during hypoxia exposure without changes in total protein content? There are several possible explanations. First, the use of mammalian antibodies may not be specific for the PDK-2 isoforms identified in fish and analyzed using qPCR. Second, although the time course for hypoxia exposures in these various studies were chosen to replicate natural durations of hypoxia exposure, it is possible that these hypoxia exposures were too short for translation of the unregulated mRNAs to occur. Thus, it is possible that had the hypoxia exposure period been longer we might have observed increased protein content. Third, increases in mRNA transcript levels for select proteins may be required to support targeting of these transcripts to the limited capacity translation machinery (45) to maintain total protein levels during hypoxia. This may be increasingly important for nuclear-encoded mitochondrial proteins where hypoxia may affect rates of mitochondrial protein degradation and import. Fourth, and possibly most intriguing, is the notion that the high levels of mRNA transcripts accumulate during hypoxia to facilitate rapid turnover of select proteins during the early part of recovery from hypoxia. Although, Lewis et al. (28) demonstrated that there was no hyperactivation of protein synthesis during recovery from hypoxia exposure in the Amazonian cichlid (*Astronatus ocellatus*), increased levels of mRNA transcripts could mean preferential synthesis of metabolically important proteins without the need to increase total protein synthesis capacity. Our experimental design included a recovery group, but the only sample taken was 12 h after hypoxia exposure ended, and therefore any rapid protein turnover would be completed. Indeed, almost all parameters measured in this recovery group, except cytoplasmic $[NAD^+]/[NADH]$ and $[ADP_{free}]$, had returned to control normoxic levels. Further research into the turnover rates of metabolically important proteins during hypoxia exposure and recovery is necessary to understand the

counterintuitive increase in mRNA expression without changing total protein.

Killifish are well known for their hypoxia tolerance (34, 48) and have an amazing capacity to activate oxygen-independent means of ATP production to survive. It is surprising however, that killifish have relatively high P_{crit} values (63.9 ± 5.6 Torr) and are oxygen conformers across a very large range of environmental oxygen tensions. The high P_{crit} value is also surprising considering their very low whole red cell Hb-P_{50} of 3.8 to 5.0 Torr (11). Our estimates of P_{crit} differ substantially from those measured in a closely related species, the gulf killifish (*F. grandis*), which had an estimated P_{crit} of ~34 Torr. The disparity in P_{crit} values could be due to species differences or differences in their physiological condition. Henriksson et al. (18) demonstrated in two species of sculpin from the family Cottidae (Pacific staghorn sculpins, *Leptocottus armatus* and Prickly sculpin, *Cottus asper*) that measures of P_{crit} are subject to change from any parameter that affects whole animal oxygen uptake (e.g., gill morphology). It is possible that differences in gill morphology or modifications to other aspects of the oxygen cascade in our killifish could impact their P_{crit}, but despite this high P_{crit} value, our fish were able to survive 15-h exposure to an enviromental O_2 tension of ~10% of their P_{crit} value. At this level of hypoxia, an animal can either attempt to sustain metabolic rate through the activation of substrate level phosphorylation or reduce metabolic rate via metabolic rate depression, and it appears that killifish employ both strategies.

Perspectives and Significance

Hypoxia survival involves a dramatic reorganization of metabolic processes to reduce ATP demands to match the limited capacity for oxygen-independent ATP production. The role of PDH in hypoxic survival has been examined extensively in carcinoma cell lines and ischemic mammalian models; however, the present study is the first to examine the complex regulation of PDH in an organism that has evolved strategies for hypoxia survival. Inactivation of PDH in killifish appears central to hypoxic survival and reaffirms the importance of limiting mitochondrial pyruvate oxidation during hypoxia to limit mitochondrial respiration and prevent ROS production and mitochondrial-mediated initiation of apoptosis. The parallels observed between killifish PDH regulation during hypoxia exposure and the responses observed in many carcinoma cell lines opens the possibility of using organisms that have evolved to survive hypoxia exposure to understand the basic biology of cancer and other hypoxia related heath issues.

GRANTS

This work was supported by grants from the Natural Sciences and Engineering Research Council of Canada to P. M. Schulte and J. G. Richards.

REFERENCES

1. **Altschul SF, Madden TL, Schaffer AA, Zhang J, Zhang Z, Miller W, Lipman DJ.** Gapped BLAST and PSI-BLAST: a new generation of protein database search programs. *Nucleic Acids Res* 25: 3389–3402, 1997.
2. **Bergmeyer HU.** *Methods of Enzymatic Analysis*. New York: Academic, 1983.
3. **Bishop T, Brand MD.** Processes contributing to metabolic depression in hepatopancreas cells from the snail *Helix aspersa J Exp Biol* 203: 3603–3612, 2000.
4. **Bishop T, St-Pierre J, Brand MD.** Primary causes of decreased mitochondrial oxygen consumption during metabolic depression in snail cells. *Am J Physiol Regul Integr Comp Physiol* 282: R372–R382, 2002.
5. **Boutilier R, Heming TA, Iwama GK.** Appendix: physicochemical parameters for use in fish respiratory physiology. In: *Fish Physiology*, edited by Hoar WS and Randall DJ. New York: Academic, 1984, p. 403–430.
6. **Bowker-Kinley MM, Davis WI, Wu P, Harris RA, Popov KM.** Evidence for existence of tissue-specific regulation of the mammalian pyruvate dehydrogenase complex. *Biochem J* 329: 191–196, 1998.
7. **Bradford MM.** A rapid and sensitive method for the quantitation of microgram quantities of protein utilizing the principle of protein-dye binding. *Anal Biochem* 72: 248–254, 1976.
8. **Buck LT, Hochachka PW.** Anoxic suppression of Na^+/K^+-ATPase and constant membrane potential in hepatocytes: support for channel arrest. *Am J Physiol Regul Integr Comp Physiol* 265: R1020–R1025, 1993.
9. **Chomczynski P, Sacchi N.** Single-step method of RNA isolation by acid quanidinium thiocyanate-phenol-chloroform extraction. *Anal Biochem* 162: 156–159, 1987.
10. **Denko NC, Fontana LA, Hudson KM, Sutphin PD, Raychaudhuri S, Altman R, Giaccia AJ.** Investigating hypoxic tumor physiology through gene expression patterns. *Oncogene* 22: 5907–5914, 2003.
11. **DiMichele L, Powers DA.** Physiological basis for swimming endurance differences between LDH-B genotypes of *Fundulus heteroclitus*. *Science* 216: 1014–1016, 1982.
12. **Dong Z, Venkatachalam MA, Wang J, Patel Y, Saikumar P, Semenza GL, Force T, Nishiyama J.** Up-regulation of apoptosis inhibitory protein IAP-2 by hypoxia. Hif-1-independent mechanisms. *J Biol Chem* 276: 18702–18709, 2001.
13. **Golding EM, Teague WE Jr., Dobson GP.** Adjustment of K′ to varying pH and pMg for the creatine kinase, adenylate kinase and ATP hydrolysis equilibria permitting quantitative bioenergetic assessment. *J Exp Biol* 198: 1775–1782, 1995.
14. **Guppy M.** The biochemistry of metabolic depression: a history of perceptions. *Comp Biochem Physiol B* 139: 435–442, 2004.
15. **Guppy M, Reeves DC, Bishop T, Withers P, Buckingham JA, Brand MD.** Intrinsic metabolic depression in cells isolated from the hepatopancreas of estivating snails. *FASEB J* 14: 999–1004, 2000.
16. **Hardewig I, Van Dijk PL, Portner HO.** High-energy turnover at low temperatures: recovery from exhaustive exercise in Antarctic and temperate eelpouts. *Am J Physiol Regul Integr Comp Physiol* 274: R1789–R1796, 1998.
17. **Hassid W, Abraham S.** Chemical procedures for analysis of polysaccharides. In: *Methods in Enzymology*, edited by Colowick S and Kaplan N. New York: Academic, 1957.
18. **Henriksson P, Mandic M, Richards J.** The osmo-respiratory compromise in sculpins: impaired gas exchange is associated with freshwater tolerance. *Physiol Biochem Zool* 81: 310–319, 2008.
19. **Hochachka PW, Buck LT, Doll CJ, Land SC.** Unifying theory of hypoxia tolerance: molecular/metabolic defense and rescue mechanisms for surviving oxygen lack. *Proc Natl Acad Sci USA* 93: 9493–9498, 1996.
20. **Holness MJ, Sugden MC.** Regulation of pyruvate dehydrogenase complex activity by reversible phosphorylation. *Biochem Soc Trans* 31: 1143–1151, 2003.
21. **Jansen MA, Shen H, Zhang L, Wolkowicz PE, Balschi JA.** Energy requirements for the Na^+ gradient in the oxygenated isolated heart: effect of changing the free energy of ATP hydrolysis. *Am J Physiol Heart Circ Physiol* 285: H2437–H2445, 2003.
22. **Katz A, Spencer MK, Sahlin K.** Failure of glutamate dehydrogenase system to predict oxygenation state of human skeletal muscle. *Am J Physiol Cell Physiol* 259: C26–C28, 1990.
23. **Kim JW, Gao P, Liu YC, Semenza GL, Dang CV.** Hypoxia-inducible factor 1 and dysregulated c-Myc cooperatively induce vascular endothelial growth factor and metabolic switches hexokinase 2 and pyruvate dehydrogenase kinase 1. *Mol Cell Biol* 27: 7381–7393, 2007.
24. **Kim JW, Tchernyshyov I, Semenza GL, Dang CV.** HIF-1-mediated expression of pyruvate dehydrogenase kinase: a metabolic switch required for cellular adaptation to hypoxia. *Cell Metab* 3: 177–185, 2006.
25. **Kramer lD, Schulte PM.** Prior PCB exposure suppresses hypoxia-induced up-regulation of glycolytic enzymes in *Fundulus heterclitus*. *Comp Biochem Physiol C* 139: 23–29, 2004.
26. **Laemmli UK.** Cleavage of structural protein during assembly of the head bacteriophage T4. *Nature* 227: 680–685, 1970.
27. **Larade K, Storey KB.** Analysis of signal transduction pathways during anoxia exposure in a marine snail: a role for p38 MAP kinase and

downstream signaling cascades. *Comp Biochem Physiol B* 143: 85–91, 2006.
28. **Lewis JM, Costa I, Val AL, Almeida-Val VM, Gamperl AK, Driedzic WR.** Responses to hypoxia and recovery: repayment of oxygen debt is not associated with compensatory protein synthesis in the Amazonian cichlid, *Astronotus ocellatus*. *J Exp Biol* 210: 1935–1943, 2007.
29. **Martinez ML, Landry C, Boehm R, Manning S, Cheek AO, Rees BB.** Effects of long-term hypoxia on enzymes of carbohydrate metabolism in the Gulf killifish, *Fundulus grandis*. *J Exp Biol* 209: 3851–3861, 2006.
30. **Mattisson A, Johansson R, Boström S.** The cellular localization of lactate dehydrogenase in skeletal muscle of eel (*Anguilla anguilla*). *Comp Biochem Physiol B* 41: 475–482, 1972.
31. **Moyes CD, Buck LT, Hochachka PW.** Temperature effects on pH of mitochondria isolated from carp red muscle. *Am J Physiol Regul Integr Comp Physiol* 254: R611–R615, 1988.
32. **Orrenius S.** Reactive oxygen species in mitochondria-mediated cell death. *Drug Metab Rev* 39: 443–455, 2007.
33. **Papandreou I, Cairns RA, Fontana L, Lim AL, Denko NC.** HIF-1 mediates adaptation to hypoxia by actively downregulating mitochondrial oxygen consumption. *Cell Metab* 3: 187–197, 2006.
34. **Powell WH, Hahn ME.** Identification and functional characterization of hypoxia-inducible factor 2α from the estuarine teleost, *Fundulus heteroclitus*: interaction of HIF-2α with two ARNT2 splice variants. *J Exp Zool* 294: 17–29, 2002.
35. **Pörtner H, Boutlier R, Tang Y, Toews D.** The use of fluoride and nitriloacetic acid in tissue acid-base physiology. II. Intracellular pH. *Respir Physiol* 81: 255–275, 1991.
36. **Pörtner H, Grieshaber MK.** Critical Po_2(s) in oxyconforming and oxyregulating animals: gas exchange, metabolic rate and the mode of energy production. In: *The Vertebrate Gas Transport Cascade: Adaptations to Environment and Mode of Life*, edited by Eduardo J and Bicudo PW. Boca Raton: CRC, 1993.
37. **Rees BB, Bowman JA, Schulte PM.** Structure and sequence conservation of a putative hypoxia response element in the lactate dehydrogenase-B gene of *Fundulus*. *Biol Bull* 200: 247–251, 2001.
38. **Richards JG, Heigenhauser GJF, Wood CM.** Glycogen phosphorylase and pyruvate dehydrogenase transformation in white muscle of trout during high-intensity exercise. *Am J Physiol Regul Integr Comp Physiol* 282: R828–R836, 2002.
39. **Richards JG, Semple JW, Bystriansky JS, Schulte PM.** Na^+/K^+-ATPase α-isoform switching in gills of rainbow trout (*Oncorhynchus mykiss*) during salinity transfer. *J Exp Biol* 206: 4475–4486, 2003.
40. **Richards JG, Wang YS, Brauner CJ, Gonzalez RJ, Patrick ML, Schulte PM, Choppari-Gomes AR, Almeida-Val VM, Val AL.** Metabolic and ionoregulatory responses of the Amazonian cichlid, *Astronotus ocellatus*, to severe hypoxia. *J Comp Physiol B* 177: 361–374, 2007.
41. **Saitou N, Nei M.** The neighbor-joining method: a new method for reconstructing phylogenetic trees. *Mol Biol Evol* 4: 406–425, 1987.
42. **Scott GR, Richards JG, Forbush B, Isenring P, Schulte PM.** Changes in gene expression in gills of the euryhaline killifish *Fundulus heteroclitus* after abrupt salinity transfer. *Am J Physiol Cell Physiol* 287: C300–C309, 2004.
43. **Semenza GL.** Oxygen-dependent regulation of mitochondrial respiration by hypoxia-inducible factor 1. *Biochem J* 405: 1–9, 2007.
44. **Semenza GL, Jiang BH, Leung SW, Passantino R, Concordet JP, Maire P, Giallongo A.** Hypoxia response elements in the aldolase A, enolase 1, and lactate dehydrogenase A gene promoters contain essential binding sites for hypoxia-inducible factor 1. *J Biol Chem* 271: 32529–32537, 1996.
45. **Smith RW, Houlihan DF, Nilsson GE, Brechin JG.** Tissue-specific changes in protein synthesis rates in vivo during anoxia in crucian carp. *Am J Physiol Regul Integr Comp Physiol* 271: R897–R904, 1996.
46. **St-Pierre J, Brand MD, Boutilier RG.** The effect of metabolic depression on proton leak rate in mitochondria from hibernating frogs. *J Exp Biol* 203: 1469–1476, 2000.
47. **St-Pierre J, Tattersall GJ, Boutilier RG.** Metabolic depression and enhanced O_2 affinity of mitochondria in hypoxic hypometabolism. *Am J Physiol Regul Integr Comp Physiol* 279: R1205–R1214, 2000.
48. **Stierhoff KL, Targett TE, Grecay PA.** Hypoxia tolerance of the mummichog: the role of access to the water surface. *J Fish Biol* 63: 580–592, 2003.
49. **Storey KB, Storey JM.** Metabolic rate depression in animals: transcriptional and translational controls. *Biol Rev* 79: 207–233, 2004.
50. **Sugden MC, Holness MJ.** Mechanisms underlying regulation of the expression and activities of the mammalian pyruvate dehydrogenase kinases. *Arch Physiol Biochem* 112: 139–149, 2006.
51. **Tamura K, Dudley J, Kumar S.** MEGA4: Molecular Evolutionary Genetics Analysis (MEGA) software version 4. *Mol Biol Evol* doi: 10.1093/molbev.msm092. 2007.
52. **Teague WE Jr, Golding EM, and Dobson GP.** Adjustment of K′ for the creatine kinase, adenylate kinase and ATP hydrolysis equilibria to varying temperature and ionic strength. *J Exp Biol* 199: 509–512, 1996.
53. **Thompson JD, Higgins DG, Gibson TJ.** CLUSTAL W: improving the sensitivity of progressive multiple sequence alignment through sequence weighting, position-specific gap penalties and weight matrix choice. *Nucleic Acids Res* 22: 4673–4680, 1994.
54. **Wang Y, Heigenhauser GJ, Wood CM.** Lactate and metabolic H^+ transport and distribution after exercise in rainbow trout white muscle. *Am J Physiol Regul Integr Comp Physiol* 271: R1239–R1250, 1996.
55. **Wang Y, Heigenhauser GJF, Wood CM.** Integrated responses to exhaustive exercise and recovery in rainbow trout white muscle: acid-base, phosphogen, carbohydrate, lipid, ammonia, fluid volume and electrolyte metabolism. *J Exp Biol* 195: 227–258, 1994.
56. **Wieser W, Krumschnabel G.** Hierarchies of ATP-consuming processes: direct compared with indirect measurements, and comparative aspects. *Biochem J* 355: 389–395, 2001.
57. **Williamson D, Lund P, Krebs H.** The redox state of free nicotinamide-adenine dinucleotide in the cytoplasm and mitochondria of rat liver. *Biochem J* 103: 514–527, 1967.
58. **Yeager DP, Ultsch GR.** Physiological regulation and conformation: a BASIC program for the determination of critical points. *Physiol Zool* 62: 888–907, 1989.